eNeuro

Research Article: New Research | Integrative Systems

Parametric representation of tactile numerosity in working memory

https://doi.org/10.1523/ENEURO.0090-19.2019

Cite as: eNeuro 2020; 10.1523/ENEURO.0090-19.2019

Received: 12 March 2019
Revised: 24 June 2019
Accepted: 2 August 2019

1. Manuscript title: Parametric representation of tactile numerosity in working memory

2. Abbreviated title: Tactile numerosity in working memory

3. Authors : Işıl Uluç [a,b], Lisa Alexandria Velenosi[a], Timo Torsten Schmidt [a], Felix Blankenburg [a,b]

[a] Neurocomputation and Neuroimaging Unit (NNU), Department of Education and Psychology, Freie Universität Berlin, 14195 Berlin, Germany

[b] Berlin School of Mind and Brain, Humboldt-Universität zu Berlin, 10099 Berlin, Germany

4. Author Contributions: IU, TTS, FB and LAV designed the research. IU, TTS and LAV programmed the experimental paradigm. IU and LAV collected the data. IU analyzed the data. IU, TTS and FB interpreted the data analysis. IU wrote the first draft of the paper with further comments from LAV, TTS and FB.

5. Correspondence should be addressed to:

Işıl Uluç

Freie Universität Berlin

Department of Education and Psychology

Neurocomputation and Neuroimaging Unit (NNU)

Habelschwerdter Allee 45 14195 Berlin

isil.uluc@fu-berlin.de

6. Number of figures: 3

7. Number of tables: 1

8. Number of multimedia: 0

9. Number of words for abstract: 161

10. Number of words for significance statement: 117

11. Number of words for introduction: 780

12. Number of words for discussion: 1237

13. Acknowledgements: Authors would like to thank Yuan-hao Wu for his assistance on data collection and Alexander von Lautz for his helpful feedback on this manuscript.

14. Conflict of interest: Authors report no conflict of interest

15. Funding sources: IU was supported by Deutscher Akademischer Austauschdienst and the Berlin School of Mind and Brain. LV was supported by the Research Training Group GRK 1589/2 by the Deutsche Forschungsgemeinschaft (DFG).

Abstract

Estimated numerosity perception is processed in an approximate number system (ANS) that resembles the perception of a continuous magnitude. The ANS consists of a right lateralized frontoparietal network comprising the lateral prefrontal cortex (LPFC) and the intraparietal sulcus. Although the ANS has been extensively investigated, only few studies focus on the mental representation of retained numerosity estimates. Specifically, the underlying mechanisms of estimated numerosity working memory (WM) is unclear. Besides numerosities, as another form of abstract quantity, vibrotactile WM studies provide initial evidence that the right LPFC takes a central role in maintaining magnitudes. In the present fMRI MVPA study in numerosity WM, we designed a delayed-match-to-numerosity paradigm to test what brain regions retain approximate numerosity memoranda. In line with parametric WM results, our study found numerosity-specific WM representations in the right LPFC as well as in the supplemental motor area and the left premotor cortex extending into the superior frontal gyrus, thus bridging the gap in abstract quantity WM literature.

Significance Statement

While the perception of approximate numerosities has been extensively investigated, research into the mnemonic representation during working memory (WM) are relatively rare. Here, we present the first study to localize WM information for approximate numerosities using functional magnetic resonance imaging (fMRI) in combination with multivariate pattern analysis (MVPA). Extending beyond previous accounts that used either a priori brain regions or electrocorticography (EEG) with poor spatial resolution and univariate analysis methods, we employed an assumption-free, time-resolved, whole-brain searchlight MVPA approach to identify brain regions which code approximate numerosity WM content. Our findings, in line with previous work, provide preliminary evidence for a higher level, modality- and format-independent abstract quantitative WM system which resides within the right lateral PFC.

Introduction

Humans can tell whether a hundred people are a larger group than fifty people quite precisely without counting. This ability to quantify amount, size, length or other analog stimulus properties can be performed non-symbolically, independent of language (Dehaene, 1992; Spitzer et al., 2014b). Indeed, human babies and several animals are able to approximate a variety of quantities (Nieder, 2005; Piazza et al., 2007, Piazza and Izard, 2009, Nieder and Dehaene, 2009), suggesting a common elemental mechanism, which has been termed the approximate number system (ANS; Gallistel and Gelman, 1992; Dehaene, 2011).

While numerosity is a discrete stimulus property, the ANS allows an approximation of numerosity, resulting in an analog estimation. Thus, in contrast to the symbolic mental representation of numbers as classes or categories, it has been hypothesized that the ANS representation resembles that of continuous quantities or magnitudes such as intensities, lengths, or frequencies (Piazza et al., 2004; Nieder and Dehaene, 2009; Spitzer et al., 2014a). In support of this, neural representations underlying both the ANS and continuous quantities have been shown to be supramodal, implying a representation abstract in nature (Piazza et al., 2006; Spitzer and Blankenburg, 2012; Spitzer et al., 2014a; Vergara et al., 2016). Moreover, small numbers are rapidly and accurately identified without counting, known as subitizing (Kaufman et al., 1949). Thus, these numbers are represented as discrete values. If the number of items exceeds the subitizing threshold, counting is required to determine the exact amount. When there is insufficient time for counting, the ANS approximates the quantity in a fast and efficient manner.

The functional anatomy of the ANS has been extensively characterized in both human and non-human primates (NHP). A frontoparietal network comprising the dorsolateral

prefrontal cortex (DLPFC) and the posterior parietal cortex (PPC), specifically the intraparietal sulcus (IPS), is involved in approximating quantities during perception (Dehaene et al., 2004; Piazza et al., 2004; 2007; Cantlon et al., 2006; 2009; Jacob and Nieder, 2009; Knops and Wilmes, 2014). Moreover, the right hemisphere has been shown to be dominant with respect to quantity estimation (Kosslyn et al., 1989; McGlone and Davidson, 1973; Young and Bion, 1979), however recent studies have found that both hemispheres respond to approximate visual numerosity (Ansari et al., 2006; Piazza et al., 2004). Particularly in non-symbolic numerosity perception, the IPS has been shown, to exhibit stronger numerosity-selective responses than the PFC (Tudusciuc and Nieder, 2009) and the PPC, and especially IPS, responds to the non-symbolic numerosity processing (Piazza et al., 2004; Piazza et al., 2007).

The ANS literature is primarily focused on perception with relatively few NHP studies extending to investigate working memory (WM) representations of approximate quantities (see Nieder, 2016). As short-term maintenance of information is critical for higher-order cognitive functions such as decision making and reasoning, it is crucial to investigate beyond perception to the maintenance of approximate quantities in WM. In line with results from perception studies of the ANS, neurons in the frontoparietal network were found, specifically in the PFC and IPS, to exhibit numerosity-selective activity during WM (Jacob et al., 2018). Furthermore, supramodal coding of numerosity memoranda in the frontoparietal cortex has been identified (see Nieder, 2017). Interestingly, in contrast to perception, the proportion of numerosity selective neurons in the PFC and their tuning strength to numerosity have been more prominent than the ones in the PPC during WM retention. Moreover, neurons in the PFC remained selective and discriminated numerosities better

than neurons in the PPC during the WM delay (Nieder and Miller, 2004; Tudusciuc and Nieder, 2009; Nieder, 2016).

To the best of our knowledge, only a single study has focused on the WM representation of numerosity in humans, although some approximate numerosity perception studies used fMRI-MVPA method with WM-related paradigms focusing on the perceptual processes instead of the WM retention (e.g., Eger et al., 2009; Borghesani, V. et al., 2018; Castaldi et al., 2019). Spitzer and colleagues (2014a) probed the oscillations underlying multimodal WM representations by training participants to estimate numerosity from sequential auditory, visual and tactile stimuli. They identified strong and long-lasting alpha oscillations in the PPC reflecting WM load whereas, in line with NHP results, beta-band activity in the right PFC showed numerosity-selective modulation.

Nevertheless, whole-brain research regarding the localization of numerosity memoranda in humans is lacking. To this end, we designed a tactile delayed-match-to-numerosity (DMTN) task in combination with whole-brain, searchlight, multivariate-pattern analysis (MVPA) of human fMRI data (e.g., Christophel et al., 2012; Schmidt et al., 2017; Uluç et al., 2018). Using this analysis approach, we localized brain regions maintaining approximate number content in WM. As per previous studies (e.g., Spitzer et al., 2014a; Nieder, 2016), we hypothesized that the content would be represented in frontal regions, specifically the right PFC.

Material and methods

Participants

38 healthy volunteers participated in the study. The sample size was based on the successful use of similar sample sizes in earlier MVPA experiments with analog experimental designs and analyses (e.g., Schmidt et al., 2017; Christophel et al., 2018). In addition, it accords with recent theoretical work on power analysis for random field theory-based cluster-level statistical inference (Ostwald et al., 2019). The data of four participants was excluded due to low performance levels (≤ 60%) resulting in data from 34 participants (age: 25.53 ± 5.43 mean years ± SD, 19 females) being further analyzed. All were right handed according to the Edinburgh Handedness Inventory with an index of 0.82 ± 0.14 (mean ± SD; Oldfield, 1971). The experimental procedure was approved by the local ethics committee and is in accordance with the Human Subject Guidelines of the Declaration of Helsinki. All participants provided written informed consent before the experiment and were compensated for their participation.

Stimuli

Tactile stimuli consisted of trains of square-wave electric pulses (200 µs) delivered via a pair of surface-adhesive electrodes attached to the participant's left wrist. A constant current neurostimulator (DS7A, Digitimer Ltd.) was used to deliver the stimuli. Subjects reported tactile sensations radiating to the thumb, index, and middle finger, verifying stimulation of the median nerve. Individual sensory thresholds were determined for each participant. The stimulus intensity was then adjusted to a target value of approximately 200% of the sensory threshold (mean: 6.42 mA, SD: 1.20 mA).

A to-be-remembered stimulus sequence comprised either 7, 9, 11, or 13 pulses. In order to dissociate stimulus length and perceived pulse frequency (spacing of tactile pulses) from the numerosity of pulses, the duration of the stimulus varied, and the inter-pulse-intervals were randomized. To this end, we defined four stimulus durations (960, 1020, 1080 and 1140 ms). Each duration was subdivided into 60 ms slots, resulting in 17, 18, 19 and 20 slots, respectively. The temporal distribution of the pulses was then randomized across the slots (see Figure 1A for illustrative stimuli). Within each run, each numerosity was presented in a short (17 or 18) and a long (19 or 20) duration resulting in 24 different numerosity-duration pairings (4 numerosities x 2 durations/run x 3 uncued numerosities). The different durations were balanced across runs. The alternatives for each cued numerosity were computed according to the respective sample (± 3 pulses). Additionally, the target stimulus and the cued sample never had the same duration ensuring that memorizing the duration or average frequency of the target does not help to perform the task. We also performed a Fourier transformation of the stimuli, which ensured that all stimuli were composed of similar combinations of frequencies. Therefore, this stimulus design ensured that participants had to memorize the stimulus numerosity since they could not use the temporal density of the pulses or the stimulus length as WM memoranda to solve the task.

Task

We employed a DMTN paradigm in which participants remembered the estimated numerosity of a stimulus. Each trial began with the presentation of two pulse sequences with different numerosities. Next, a retro-cue (“1” or “2”) indicated which of the two numerosities had to be remembered. To suppress potential perceptual residues, in the sense of afterimages (e.g. Sperling, 1960; Christophel and Haynes, 2014; Christophel et al., 2015), a mask consisting of the longest duration (1140 ms) with a pulse in each of the 20 slots, was

applied simultaneously with the onset of the retro-cue. Following a 12 s retention phase, two test stimuli were presented and a two-alternative forced-choice was given. Neither of the test stimuli were identical to the encoded stimulus, however, one had the same numerosity while the duration and the frequency were different. This ensured that participants used the approximated numerosity of the stimulus instead of some other stimulus feature to correctly match the test with the remembered stimulus. The numerosity of the alternative stimulus was 3 pulses ± the target stimulus. To ensure that the number of pulses in a sequence could not be easily counted, the lower alternative stimulus for the lowest to-be-remembered numerosity (7), was set to five (5) and thus above a previously established subitizing threshold of around four (for tactile modality, it was shown to be 3-4; e.g., Riggs et al., 2006; Plaisier et al., 2009; 2010; 2011; Spitzer et al., 2014a; Tian & Chen, 2018). After the second target stimulus, participants had 1.5 s to indicate, via button-press with their right middle or index finger, which of the two stimuli had the same numerosity as the encoded stimulus (see Figure 1B for experimental design). Furthermore, the response mapping was counter-balanced across participants. In total, a trial lasted 21 s and an experimental run, consisting of all possible stimulus pairings presented equally often (12 pairings x 4 presentations = 48 trials) in a randomized order, with inter-trial intervals of 1.5 or 3.5 s, lasted 18.7 minutes. Four experimental runs were collected for each participant, resulting in a total recording time of 74.8 minutes.

Prior to the fMRI experiment, each participant was familiarized with the timing and structure of the task by performing up to two experimental runs outside the scanner.

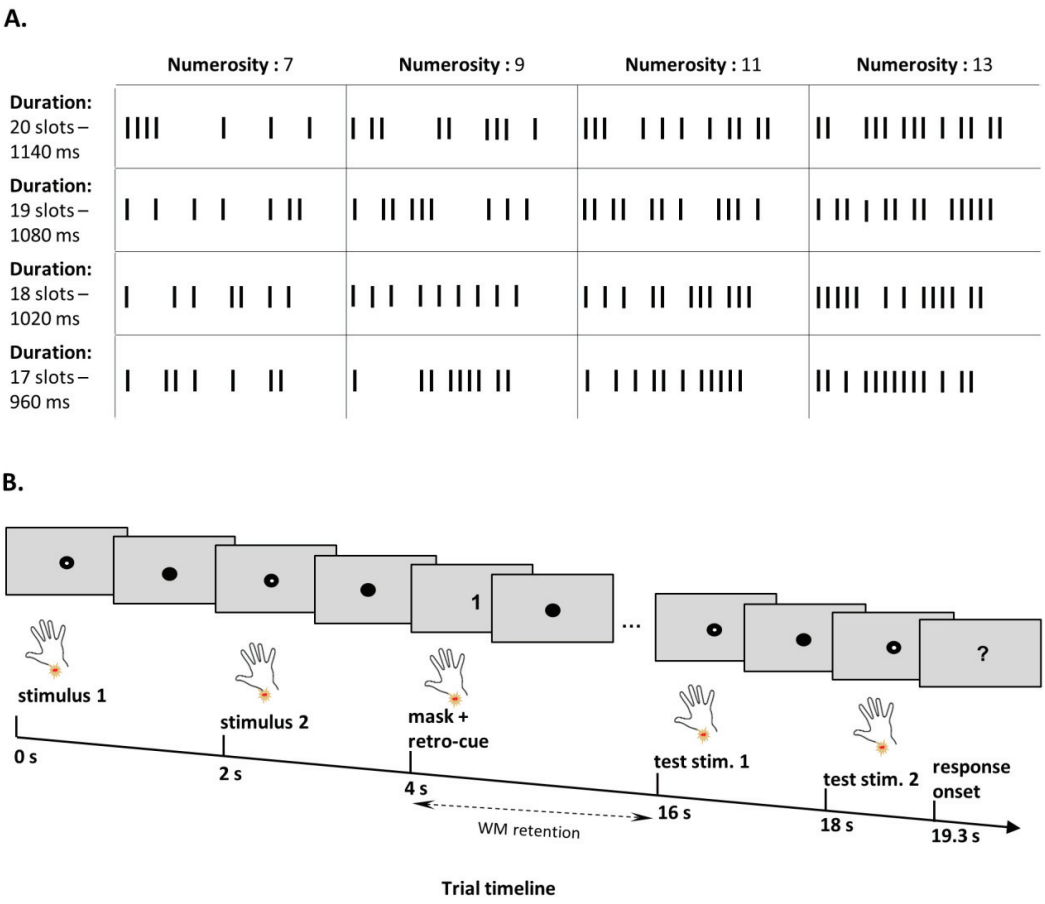

Figure 1. Sample pulse sequences and experimental paradigm **A.** Sample Stimuli. Pulse sequences of 7, 9, 11 and 13 were used as experimental stimuli. For each numerosity, there were four different durations (960, 1020, 1080 and 1140 ms), where each duration was sub-divided into 60 ms slots. The distribution of pulses to slots was randomized for each stimulus presentation. The first and the last slot of each stimulus always contained a pulse. The stimuli displayed are for illustrative purposes. **B.** Experimental paradigm. A delayed-match-to-numerosity task was employed, where two sample stimuli and a mask were presented consecutively. A visual retro-cue presented simultaneously with the mask indicated which of the numerosities should be retained for the 12 s delay. After the delay, participants performed a two-alternative forced-choice, indicating which of the two test stimuli had the same numerosity as the cued stimulus. The response period was 1.5 s. Please note that the stimulus duration and inter-stimulus-interval changed depending on the stimulus duration, but the onset of each event was locked to coincide with the onset of an image acquisition.

Number naming test assessing countability

Subsequent to the fMRI session, we applied a number naming task to ensure that participants were unable to count the number of pulses employed in the stimulus set. Participants were asked to try to count the number of pulses. The stimuli ranged from 1 to 15 pulses with 5 different duration and temporal pulse distribution combinations of each

numerosity tested, resulting in 75 trials. The counting test was performed after fMRI data acquisition so as to prevent biasing the participants towards counting the pulses in the main experiment.

To ensure that the presented numerosities were above participants' subitizing thresholds, we calculated the mean performance for each numerosity across participants and calculated each average estimated numerosity. We then compared the slope of accuracy for estimating numerosities with earlier studies that calculated subitizing thresholds for tactile stimuli (Riggs et al., 2006; Plaisier et al., 2009; 2010; 2011; Spitzer et al., 2014a; Tian & Chen, 2018). We performed a linear trend analysis using linear regression to determine whether the distance between the true and estimated numerosity scales with increasing true numerosity in a linear fashion.

fMRI data acquisition and pre-processing

fMRI data were acquired in 4 runs, with a Siemens 3 T Tim Trio MRI scanner (Siemens, Erlangen) equipped with a 32-channel head coil. In each run, 565 images were collected (T2*-weighted gradient-echo EPI: 37 slices; ascending order; 20% gap; whole brain; TR = 2000 ms; TE = 30 ms; 3 x 3 x 3 mm^3; flip angle = 70°; 64 x 64matrix). After the last functional run, a high-resolution structural scan was recorded using a T1-weighted MPRAGE sequence (1 x 1 x 1 mm^3; TR = 1900 ms; TE = 2.52 ms; 176 sagittal slices).

fMRI data preprocessing was performed using SPM12 (Wellcome Trust Centre for Neuroimaging, Institute for Neurology, University College London, London, UK). Functional images were slice-time corrected and spatially realigned to the mean image. In order to conserve the spatiotemporal structure of the fMRI data for the multivariate analyses, no smoothing or normalization was performed. For the univariate control analysis, functional images were normalized to MNI-space and smoothed with an 8 mm FWHM kernel.

First Level Finite Impulse Response Models

A time-resolved, multivariate searchlight analysis (Kriegeskorte et al., 2006, Schmidt et al., 2017) was used to identify brain regions encoding memorized numerosity information. First, a general linear model (GLM) with a set of finite-impulse-response (FIR) regressors was fit to each participant's data to obtain run-wise parameter estimates of each WM content (numerosity value of 7, 9, 11 or 13). A single FIR regressor was estimated for each fMRI image or 2 s time bin (1 TR), thus, the 20 s trial was divided into 10 time bins. We additionally included the first five principal components accounting for the most variance in the cerebrospinal fluid (CSF) and white matter signal time courses respectively (Behzadi et al., 2007), and six head motion regressors, as regressors of no interest. Moreover, the data was filtered with a high-pass filter of 128 s. The resulting parameter estimates were used for the MVPA performed with The Decoding Toolbox v. 3.52 (TDT) (Hebart et al., 2015).

Multivariate Pattern Analysis

For the decoding of memorized numerosity information, a searchlight-based multivariate analysis using a support vector regression (SVR) approach was performed with the computational routines of LIBSVM (Chang and Lin, 2011), as implemented in TDT. SVR MVPA (see Kahnt et al., 2011 for more discussion; Schmidt et al., 2017) considers the variable of interest (memorized numerosity) as a continuous data vector with multiple independent variables (multi-variate BOLD activities) as opposed to the commonly used support vector machine approach that treats the variable of interest as a categorical object. This means that the SVR MVPA approach seeks a linear continuum for the numerosities in which their distance is proportional to the distances of the rank order.

We analyzed each time bin independently by implementing a searchlight decoding analysis with a spherical searchlight radius of 4 voxels. For a given voxel, z-scaled parameter estimates (across samples) corresponding to each WM condition were extracted from all voxels within the spherical searchlight for each run. This yielded 16 pattern vectors (4 WM contents x 4 runs), each corresponding to the BOLD activity pattern for a specific WM condition of a functional run. We then fitted a linear function to these pattern vectors such that the multivariate distribution for the different numerosities follows a linear mapping of numerosities. The z-scaled parameter estimates were entered into an SVR model with a fixed regularization parameter c that was set to 1.

We used a leave-one-run-out cross-validation scheme for the subject-level decoding analysis. The SVR classifier was trained on three runs (12 pattern vectors) and tested on the data of the independent fourth run (4 pattern vectors) for how well it predicted the values of the remaining run. The allocation of training and test runs was iterated so that each of the four functional runs was used as a test run once, resulting in four cross-validation folds. The prediction performance from each cross-validation fold was reported by a Fisher's z-transformed correlation coefficient between the predicted and the actual numerosity information estimate. The mean prediction accuracy across cross-validation folds was assigned to the center voxel of the searchlight, and the center of the searchlight was moved voxel by voxel through the brain, resulting in a whole-brain prediction accuracy map. Consequently, we obtained one prediction accuracy map for each time bin for each participant, where the prediction accuracy reflects how well a linear ordering according to the associated numerosities could be read out from the locally distributed BOLD activity pattern at a given voxel location and time.

Next, prediction accuracy maps were normalized to MNI space and smoothed with an 8 mm FWHM kernel. They were then entered into a second-level, repeated measures ANOVA analysis with subject and time (time bins) as factors. To assess which brain regions exhibit WM content-specific activation patterns during the delay period, we computed a t-contrast across the 6 time bins corresponding to the 12 s WM delay (time bins 3-8). The results are presented at $p < 0.05$ family-wise error correction (FWE) at the cluster level with a cluster-defining threshold of $p < 0.001$. Cytoarchitectonic references are based on the SPM anatomy toolbox where possible (Eickhoff et al., 2005). Presented images, e.g. surface projections with applied color scales were created using MRIcron version9/9/2016 (McCausland Center for Brain Imaging).

Control analyses

In the first control analysis, we examined whether the decoded numerosity information during WM retention was specific to WM or could be assigned to perceptual residues. To this aim, we defined a second, first-level model with FIR regressors for the non-memorized stimulus. We then implemented the identical searchlight decoding procedure as the main analysis. Thus, this control analysis tested for the presence of numerosity information of the non-memorized stimulus.

Next, we conducted a parametric univariate analysis to ensure that the decoded information in the main analysis is not due to the modulation of mean activity level. To this end, we fitted a standard GLM with 4 HRF-convolved regressors: one regressor to capture WM processes, a parametrically-modulated regressor for the numerosity content of the WM memoranda as well as 8 (4 numerosities x 2 (sample, test)) additional parametrically-modulated regressors for each sample and test stimulus. First-level baseline contrasts for

the parametric effect of memorized numerosity were forwarded to a second-level one-sample t-test.

Finally, to test the specificity of the SVR analysis to the parametric order of the four numerosities, we performed exhaustive whole-brain SVR searchlight analyses for all possible permutations of numerosity labels. In order to achieve this, we computed distance rank order as a sum of the absolute difference of adjacent ranks (e.g., 11, 13, 7, 9 numerosity, is distance 5 (|3-4|+|4-1|+|1-2|) for all possible permutations of the numerosity-order. Then, the permutations were grouped according to their distance from the original rank order. We used 12 instead of 24 permutations as the distances of rank order permutations are symmetric. Including the permutation with the correct linear order, the 12 permutations are aggregated into five classes depending on their distance from the correct linear order. Then, for each permutation analysis, we extracted the prediction accuracies of the group-peak voxels that are defined in the original analysis. For statistical assessment, we calculated the mean prediction accuracy across related time bins (WM time bins 3-8) for each peak voxel for each distance group (Figure 3C).

Results

Behavioral performance

Determined on the basis of earlier MVPA experiments and our behavioral pilots, 34 participants performed with 65.36 ± 3.29% (mean ± SD) accuracy in the demanding DMTN task across the four experimental runs (see Figure 2A). To test whether the behavioral performance differed for the four numerosity values, we performed a one-way repeated measures ANOVA with four levels, one for each numerosity. This test revealed a significant main effect ($F(3,135)=7.52$, $p<0.001$). Post-hoc t-tests (Bonferroni-corrected for multiple comparisons) between performances were significant for numerosity values 7 and 13 and 9 and 13 ($p < 0.05/6$; see Figure 2A). This is expected because we did not control for the Weber-Fechner effect except for the lowest numerosity (which we did due to subitizing concerns). As a result, as the numerosity increases, it becomes more difficult to differentiate between the sample and alternative stimuli, thus resulting in a lower performance for high numerosities (Fechner, 1966) but is unlikely to affect WM processing.

Behavioral performance on number naming test assessing countability

To test whether participants were able to count the numerosities employed in the current study, participants performed an additionally number naming test. Previous research in tactile numerosity indicated the subitizing threshold for comparable stimuli to be 4 pulses (Riggs et al., 2006; Plaisier et al., 2009; 2010; 2011; Spitzer et al., 2014a; Tian & Chen, 2018). The approximation of the subitizing threshold identified in the present study is in line with these reports (Figure 2B). As expected, participants' perceptual accuracy decreased with increasing numerosity and performance decreased to 50% when more than 3 pulses were

presented. Similarly, the distance between the true and estimated numerosity increased with increasing numerosities ($p < 0.001$, linear trend analysis) (Figure 2C).

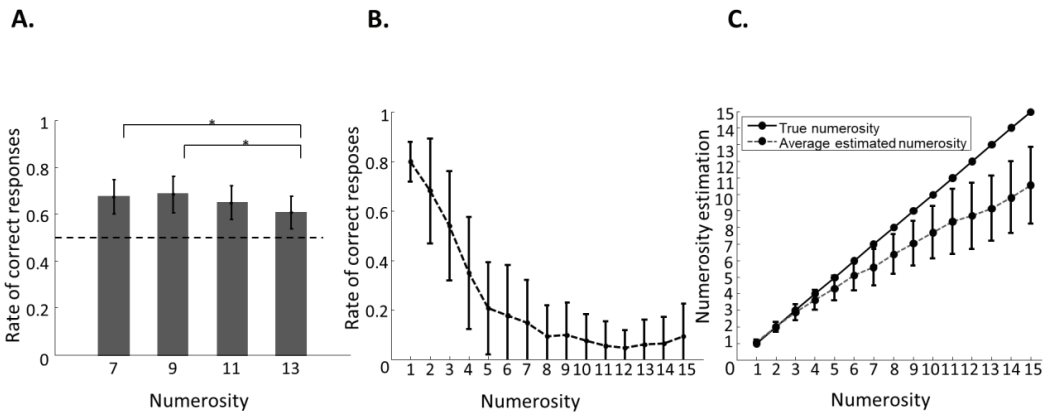

Figure 2. A. Mean rate of correct responses across participants (n = 34) for different numerosities in main WM DMTN task. The figure shows that the WM performance decreases with increasing numerosity. Error bars represent standard deviation (SD). Asterisks indicate statistical significance for pair-wise t-tests, Bonferroni corrected for multiple comparisons ($p < 0.05/6$). **B.** Mean performance across subjects for estimated numerosity in number naming task (mean ± SD). **C.** True numerosities vs. mean numerosity estimations (error bars show SD).

Multivariate mapping of regions that code numerosity as WM content

The time-resolved, searchlight-based multivariate regression analysis was performed to identify brain regions representing estimated numerosity memoranda. The SVR MVPA analysis for the WM retention period revealed numerosity-specific responses in the left PMC, left middle frontal gyrus (MFG), left superior frontal gyrus (SFG) extending into bilateral supplementary motor areas (SMA), right SFG extending to the right frontal pole and right MFG extending into the pars triangularis of the right IFG. Results are reported at $p < 0.05$, FWE-corrected at the cluster level with a cluster-defining threshold of $p < 0.001$ (Figure 3 and Table 1).

For the sake of completeness, we investigated whether numerosity information could be decoded from the IPS at an uncorrected statistical threshold of $p < 0.001$. We found a cluster in the right PPC extending to the IPS (peak at MNI x = 36, y = -52, z = 36 mm, z-score =

359 3.89, k = 164), which was identified as hIP1 with a 39.5% probability and hIP3 with a 5.9%

360 probability using the SPM anatomy toolbox (Eickhoff et al., 2005) at $p_{uncorrected} < 0.001$.

361

362

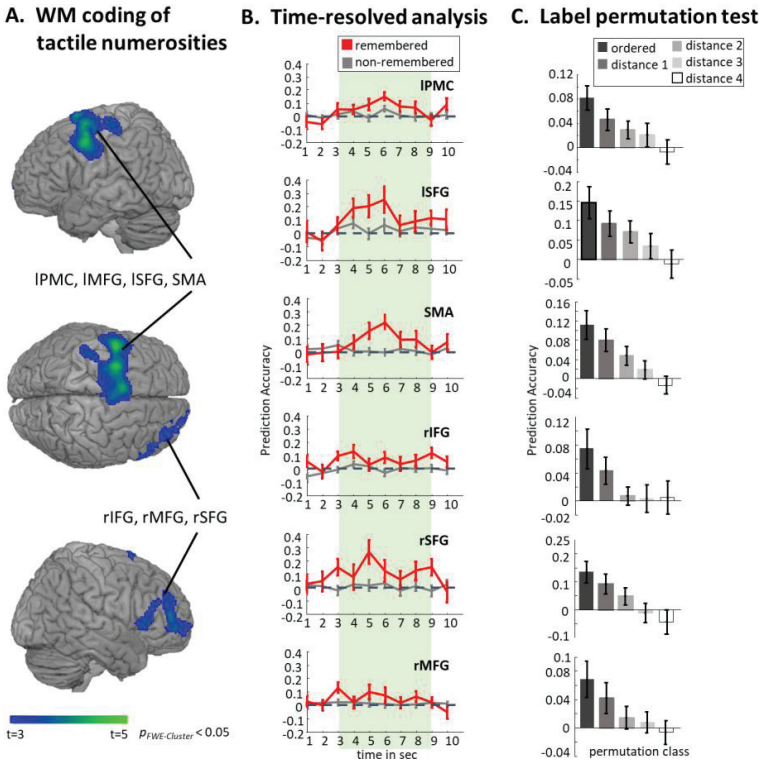

363

Figure 3. A. Brain regions coding information for the memorized estimated numerosities. Group level results of a t-contrast testing the 12 s WM delay for above chance prediction accuracy. Brain regions carrying information about memorized scalar magnitudes are: IFG = inferior frontal gyrus, MFG = middle frontal gyrus, PMC = premotor cortex, SMA = supplementary motor area, SFG = superior frontal gyrus. **B.** Time-courses of decoding accuracies of remembered (red) and non-remembered (grey) stimuli for all identified brain regions in the main analysis (Fig. 3A). Error bars indicate standard error. The figure shows that, for all clusters depicted in the main analysis, there is more numerosity-specific WM information for the remembered than forgotten numerosity and the information is present throughout the WM delay period. **C.** Results of the label-permutation tests. 5 bars are shown for each brain region, respectively. Each bar displays the mean prediction accuracy estimated from the distance to correct order groups. The shade of the bar color, ranging from black to white, depicts the different distance to correct ordering. Black bars indicate the mean prediction performance of the group with the correct linear order, while white bars represent the mean prediction accuracy derived from the most linearly unordered data. Brain regions tested for label permutation are: IFG = inferior frontal gyrus, MFG = middle frontal gyrus, PMC = premotor cortex, SMA = supplementary motor area, SFG = superior frontal gyrus. Error bars indicate standard error of the mean.

364

Table 1. SVR MVPA results for tactile numerosity WM task

Anatomical label and MNI coordinates of brain areas depicting memorized numerosity information during WM. All results are reported at $p_{FWE\text{-}Cluster} < 0.05$ with a cluster-defining threshold of $p < 0.001$. Mean prediction accuracy over the delay period is reported. Areas were, where possible, identified using the SPM anatomy toolbox (Eickhoff et al., 2005). IFG = inferior frontal gyrus, MFG = middle frontal gyrus, PMC = premotor cortex, MI = primary motor cortex, SMA = supplementary motor area, SFG = superior frontal gyrus.

Cluster size	Anatomical region	Peak MNI coordinates			z-score	Prediction accuracy
		X	Y	Z		
4557	Left PMC/MI	-50	2	52	4.78	0.082
	Left SFG	-28	0	60	7.74	0.146
	SMA	-6	10	74	4.48	0.114
1342	Right SFG	32	50	10	4.17	0.135
	Right IFG (pars triangularis)	60	24	2	4.17	0.075
	Right MFG	40	50	30	3.69	0.069

Control analyses

To test, if the identified decoded information is indeed specific to the memorized numerosity representation, we applied the same searchlight procedure to the non-memorized numerosity stimulus. This analysis did not reveal any clusters with above-chance prediction accuracy at $p_{FWE\text{-}Cluster} < 0.05$.

Additionally, we conducted a univariate parametric analysis to test whether the decoding results could be due to differences in activation strength between WM contents. A second level t-test revealed no significant voxels at $p_{FWE\text{-}Cluster} < 0.05$, thus providing evidence for the multivariate nature of the numerosity representations identified in this study rather than the modulation of univariate mean activity.

Finally, we performed label-permutation tests in order to ensure the specificity of the linear ordering of stimuli in the SVR MVPA. Higher prediction accuracies were expected

when the activation patterns in a given brain region represented the correct order of the four numerosity labels, and it was expected to decrease with the distance from the correct ordering. As expected, the prediction accuracy during WM was the highest for the true-labelled data and decreased with increasing distance from the correct ordering (Figure 3C).

Discussion

The current study, to our knowledge, is the first to identify brain regions that code approximate numerosity WM content using human neuroimaging methods. Thus, this study extends the extensive literature on ANS perception to the maintenance of mental representations which can be used for higher-order cognitive functions. We employed a well-established, whole-brain, searchlight, DMTN paradigm to identify representations of tactile approximate numerosity memoranda. Specifically, we employed an SVR technique, which in contrast to support vector machines, treats the retained WM content as a continuous variable and thus predicts the ordering of content along the variable, rather than a singularly specific class label. Consequently, an above-chance prediction accuracy in a brain region means that the content-specific activation patterns follow a linear ordering according to the associated numerosity. Our searchlight analysis identified a distributed network spanning the left PMC, bilateral SFG, bilateral SMA and right MFG extending into right IFG. Therefore, these regions contain linearly-ordered, multivariate WM representations of the numerosities.

Our results are in line with previous numerosity WM studies in NHPs and human EEG which have established the central role of the PFC. Indeed, previous uni- and multimodal studies have identified content-specific representations in the PFC (Nieder and Miller, 2004; Tudusciuc and Nieder, 2009; Nieder, 2016; Spitzer et al., 2014a; Jacob et al., 2018). More specifically, in humans, parametric modulation of upper-beta oscillations in the right lateral PFC has been shown to reflect analog numerosity estimation which has been derived from discrete sequences, both within and between stimulus modalities (Spitzer et al., 2014a). Thus, the numerosity representations in the PFC are likely to be supramodal in nature.

However, those studies used either electrophysiological recordings from an a priori brain region or EEG and have employed univariate data analysis methods. The present study extends the literature on numerosity WM in two ways: firstly, to whole-brain fMRI data, and secondly to multivariate data analysis methods, specifically the SVR MVPA. The benefits of multivariate over univariate analysis methods have been well-established (e.g., Haynes, 2015). Multivariate analysis techniques are sensitive to the combinatorial aspects of voxel activity, thereby enabling the identification of spatially distributed representations (e.g., Haynes, 2015; Hebart and Baker, 2018). Thus, our results agree with and extend the previous NHP and human EEG numerosity WM findings to whole-brain, spatially distributed activity patterns, suggesting that estimated numerosity WM content is maintained in the LPFC (Nieder et al., 2002; Nieder and Miller, 2003; 2004; Tudusciuc and Nieder, 2009; Nieder, 2016; Spitzer et al., 2014a).

It should be noted that we used temporally distributed tactile numerosity stimuli as the WM memoranda, namely the numerosity was presented as a sequence of pulses. Evidence exists for potential differences in perceptual processing of spatially- and temporally-distributed numerosities, where spatially-distributed stimuli appear to be processed in parietal regions while temporarily-distributed stimuli do not (Cavdaroglu and Knops, 2018). In line with the finding of Cavdaroglu and Knops (2018), we used temporally distributed stimuli did not find evidence of WM representations in posterior regions in our full brain FWE corrected analysis. However, a small cluster (k=164) extending to right IPS was observed to represent remembered numerosity content at an uncorrected threshold of $p < 0.001$. While our results agree with numerosity WM findings in NHPs that suggest frontal rather than parietal coding for spatial numerosity stimuli during WM retention (for review, see Nieder, 2016) further investigation is needed to conclusively decide for the role of the

IPS. The role of the IPS could be interpreted as specific to perceptual processing, and therefore only revealed at a lower threshold in our analysis, while the PFC contains WM instead. Alternatively, a potentially different nature of the neuronal code, e.g. spatial distribution of a multivariate code, in the IPS might lead to the observed findings (see Hebart and Baker, 2018). That is, it might be the temporarily-distributed nature of the applied stimuli that drives the effects in the PFC, and the IPS would be more specialized for spatially distributed presentations as used by most previous studies. A future direct comparison of our results with spatial numerosity stimuli is necessary to test for differences determined by the stimulus types.

Moreover, while the literature relating to numerosity WM is limited, there is extensive work exploring the WM representation of abstract quantities more generally. Specifically, the frequency discrimination task has been systematically explored in a multitude of modalities with a wide range of methods (e.g., Romo et al., 1999; Spitzer at al., 2010; Lemus et al., 2009; Spitzer & Blankenburg, 2011; 2012; Fassihi et al., 2014; Vergara et al., 2016; von Lautz et al., 2017; Schmidt et al., 2017; Wu et al., 2018; Uluç et al., 2018). Numerosity and frequency share several traits, particularly they are both abstract magnitudes which may be represented in a supramodal fashion (Spitzer and Blankenburg, 2012; Vergara et al., 2016; Nieder, 2016; Miller, 2003). However, whether their underlying WM representations are maintained by a shared network has yet to be explored. The present study provides an initial step towards resolving this question by providing the first evidence that frequency and numerosity WM representations are maintained in overlapping brain regions. We identified numerosity-specific WM content in the right IFG, SMA and left PMC which is in agreement with results from frequency studies also using an fMRI-MVPA approach in humans (Schmidt et al., 2017; Wu et al., 2018; Uluç et al., 2018). Uni- and multimodal research in both NHPs

and humans has identified frequency-specific content in the right LPFC and SMA thereby suggesting the WM representations are modality independent in nature (e.g., Romo et al., 1999; Hernandez et al., 2002; 2010; Barak et al., 2010; Spitzer et al., 2010; Spitzer & Blankenburg, 2011; 2012; Vergara et al., 2016; Schmidt et al., 2017; Wu et al., 2018). However, the explicit relationship between frequency and numerosity still needs to be explored, particularly with respect to the underlying neural codes of numerosity and frequency representations (see Nieder, 2017).

Additionally, we identified numerosity-specific content in the left PMC. Previous findings from frequency WM fMRI-MVPA studies identified abstract quantity information in the PMC (Schmidt et al., 2017; Wu et al., 2018; Uluç et al., 2018). Moreover, the dorsal PMC has been shown to represent abstract numerical rules, such as comparison and calculation (Gruber et al., 2001; Eger et al., 2003; Nieder, 2005). This is in line with the present task which required the comparison of numerical quantities, suggesting representation of task-relevant, numerosity-specific information to be used in numerical comparison.

In summary, the data at hand is in line with the suggestion of a domain general, abstract magnitude processing system. This abstract processing system can be identified by multivariate WM representations of tactile numerosity stimuli within the right PFC. Taken together with previous findings which found WM representations of tactile frequency (Spitzer et al., 2010; Spitzer and Blankenburg, 2012; Spitzer et al., 2014a; Schmidt et al., 2017; Wu et al., 2018), visual flicker frequency (Spitzer and Blankenburg, 2012; Spitzer et al., 2014a; Wu et al., 2018), and auditory frequency (Spitzer and Blankenburg 2012, Uluç et al., 2018), and the reports of number coding (Nieder et al., 2002; Nieder and Miller, 2003; 2004; Tudusciuc and Nieder, 2009; Nieder, 2016) in the PFC, the present study provides additional evidence suggesting that the PFC is capable of representing both analog quantities as well as

parametric stimulus properties as frequencies. Thus, we provide preliminary evidence for a higher level, modality- and format-independent abstract quantitative WM system which resides within the PFC.

References

Ansari, D., Dhital, B., Siong, S.C. (2006). Parametric effects of numerical distance on the intraparietal sulcus during passive viewing of rapid numerosity changes. *Brain Res. 1067*, 181–188.

Barak, O., Tsodyks, M., & Romo, R. (2010). Neuronal population coding of parametric working memory. *The Journal of Neuroscience : The Official Journal of the Society for Neuroscience*, *30*(28), 9424–30. http://doi.org/10.1523/JNEUROSCI.1875-10.2010

Behzadi, Y., Restom, K., Liau, J., & Liu, T. T. (2007). A component based noise correction method (CompCor) for BOLD and perfusion based fMRI. *NeuroImage, 37*(1), 90–101. http://doi.org/10.1016/j.neuroimage.2007.04.042

Borghesani, V., Dolores de Hevia, M., Viarouge, A., Chagas, P. P., Eger, E., & Piazza, M. (2018). Processing number and length in the parietal cortex: Sharing resources, not a common code. *Cortex*. doi:10.1016/j.cortex.2018.07.017

Cantlon, J. F., Brannon, E. M., Carter, E. J., & Pelphrey, K. A. (2006). Functional Imaging of Numerical Processing in Adults and 4-y-Old Children. PLoS Biology, 4(5), e125. https://doi.org/10.1371/journal.pbio.0040125

Cantlon, J. F., Platt, M. L., & Brannon, E. M. (2009). Beyond the number domain. Trends in Cognitive Sciences, 13(2), 83–91. https://doi.org/10.1016/j.tics.2008.11.007

Castaldi, E., Piazza, M., Dehaene, S., Vignaud, A., & Eger, E. (2019). Attentional amplification of neural codes for number independent of other quantities along the dorsal visual stream. *bioRxiv*, 527119. https://doi.org/10.1101/527119

Cavdaroglu, S., & Knops, A. (2018). Evidence for a Posterior Parietal Cortex Contribution to Spatial but not Temporal Numerosity Perception. Cerebral Cortex. https://doi.org/10.1093/cercor/bhy163

Chang, C.-C., & Lin, C.-J. (2011). LIBSVM. *ACM Transactions on Intelligent Systems and Technology*, *2*(3), 1–27. http://doi.org/10.1145/1961189.1961199

Christophel, T. B., Hebart, M. N., & Haynes, J.-D. (2012). Decoding the contents of visual short-term memory from human visual and parietal cortex. *The Journal of Neuroscience : The Official Journal of the Society for Neuroscience*, *32*(38), 12983–9. http://doi.org/10.1523/JNEUROSCI.0184-12.2012

Christophel, T.B., Haynes, J.-D. (2014). Decoding complex flow-field patterns in visual working memory. *Neuroimage 91*, 43–51. doi:10.1016/j.neuroimage.2014.01.025

514 Christophel, T.B., Cichy, R.M., Hebart, M.N., Haynes, J.-D. (2015). Parietal and early visual
515 cortices encode working memory content across mental transformations. *Neuroimage*
516 *106*, 198–206. doi:10.1016/j.neuroimage.2014.11.018

517 Christophel, T. B., Allefeld, C., Endisch, C., & Haynes, J.-D. (2018). View-Independent Working
518 Memory Representations of Artificial Shapes in Prefrontal and Posterior Regions of the
519 Human Brain. *Cerebral Cortex*, *28*(6), 2146–2161.
520 https://doi.org/10.1093/cercor/bhx119

521 Dehaene, S. (1992). Varieties of numerical abilities. *Cognition, 44*(1–2), 1–42.
522 https://doi.org/10.1016/0010-0277(92)90049-N

523 Dehaene, S., Molko, N., Cohen, L., & Wilson, A. J. (2004). Arithmetic and the brain. *Current*
524 *Opinion in Neurobiology*, *14*(2), 218–224. https://doi.org/10.1016/J.CONB.2004.03.008

525 Dehaene, S. (2011). *The number sense: How the mind creates mathematics* (Rev. and
526 updated ed.). New York, NY, US: Oxford University Press.

527 Eger, E., Sterzer, P., Russ, M. O., Giraud, A.-L., & Kleinschmidt, A. (2003). A Supramodal
528 Number Representation in Human Intraparietal Cortex. *Neuron, 37(4),* 719–726.
529 https://doi.org/10.1016/S0896-6273(03)00036-9

530 Eger, E., Michel, V., Thirion, B., Amadon, A., Dehaene, S., & Kleinschmidt, A. (2009).
531 Deciphering Cortical Number Coding from Human Brain Activity Patterns. *Current*
532 *Biology, 19*(19), 1608–1615. https://doi.org/10.1016/J.CUB.2009.08.047

533 Eickhoff, S. B., Stephan, K. E., Mohlberg, H., Grefkes, C., Fink, G. R., Amunts, K., & Zilles, K.
534 (2005). A new SPM toolbox for combining probabilistic cytoarchitectonic maps and
535 functional imaging data. *NeuroImage*, *25*(4), 1325–35.
536 http://doi.org/10.1016/j.neuroimage.2004.12.034

537 Fassihi, A., Akrami, A., Esmaeili, V., & Diamond, M. E. (2014). Tactile perception and working
538 memory in rats and humans. *Proceedings of the National Academy of Sciences of the*
539 *United States of America*, *111*(6), 2331–6. https://doi.org/10.1073/pnas.1315171111

540 Fechner, G. (1966). *Elements of Psychophysics*. New York: Holt Rinehart & Winston.

541 Gallistel, C. R., & Gelman, R. (1992). Preverbal and verbal counting and computation.
542 *Cognition, 44*(1–2), 43–74. https://doi.org/10.1016/0010-0277(92)90050-R

543 Gruber, O., Indefrey, P., Steinmetz, H., & Kleinschmidt, A. (2001). Dissociating Neural
544 Correlates of Cognitive Components in Mental Calculation. *Cerebral Cortex*, *11*(4), 350–
545 359. https://doi.org/10.1093/cercor/11.4.350

546 Haynes, J.-D. (2015). A Primer on Pattern-Based Approaches to fMRI: Principles, Pitfalls, and
547 Perspectives. *Neuron, 87*(2), 257–270. https://doi.org/10.1016/J.NEURON.2015.05.025

548 Hebart, M. N., Görgen, K., & Haynes, J.-D. (2015). The Decoding Toolbox (TDT): a versatile
549 software package for multivariate analyses of functional imaging data. *Frontiers in*
550 *Neuroinformatics*, *8*. http://doi.org/10.3389/fninf.2014.00088

551 Hebart, M. N., & Baker, C. I. (2018). Deconstructing multivariate decoding for the study of
552 brain function. *NeuroImage, 180*(Pt A), 4–18.
553 https://doi.org/10.1016/j.neuroimage.2017.08.005

554 Jacob, S. N., & Nieder, A. (2009). Tuning to non-symbolic proportions in the human
555 frontoparietal cortex. *European Journal of Neuroscience, 30*(7), 1432–
556 1442. https://doi.org/10.1111/j.1460-9568.2009.06932.x

557 Jacob, S. N., Hähnke, D., & Nieder, A. (2018). Structuring of Abstract Working Memory
558 Content by Fronto-parietal Synchrony in Primate Cortex. Neuron, 99(3), 588–
559 597.e5. https://doi.org/10.1016/j.neuron.2018.07.025

560 Kahnt, T., Heinzle, J., Park, S. Q., & Haynes, J.-D. (2011). Decoding different roles for vmPFC
561 and dlPFC in multi-attribute decision making. *NeuroImage, 56(*2), 709–
562 715. https://doi.org/10.1016/j.neuroimage.2010.05.058

563 Kaufman, E. L., Lord, M. W., Reese, T. W., & Volkmann, J. (1949). The Discrimination of Visual
564 Number. *The American Journal of Psychology*, *62*(4), 498.
565 https://doi.org/10.2307/1418556

566 Knops, A., & Willmes, K. (2014). Numerical ordering and symbolic arithmetic share frontal
567 and parietal circuits in the right hemisphere. NeuroImage, 84, 786–
568 795. https://doi.org/10.1016/J.NEUROIMAGE.2013.09.037

569 Kosslyn, S.M., Koenig, O., Barrett, A., Cave, C.B., Tang, J., Gabrieli, J.D. (1989). Evidence for
570 two types of spatial representations: hemispheric specialization for categorical and
571 coordinate relations. *J. Exp. Psychol. Hum. Percept. Perform. 15*, 723–735.

572 Kriegeskorte, N., Goebel, R., & Bandettini, P. (2006). Information-based functional brain
573 mapping. *Proceedings of the National Academy of Sciences of the United States of*
574 *America*, *103*(10), 3863–8. http://doi.org/10.1073/pnas.0600244103

575 Lemus, L., Hernández, A., & Romo, R. (2009). Neural encoding of auditory discrimination in
576 ventral premotor cortex. *Proceedings of the National Academy of Sciences of the United*
577 *States of America*, *106*(34), 14640–5. https://doi.org/10.1073/pnas.0907505106

578 McGlone, J., Davidson, W. (1973). The relation between cerebral speech laterality and spatial
579 ability with special reference to sex and hand preference. *Neuropsychologia 11*, 105–
580 113.

581 Nieder, A., Freedman, D. J., & Miller, E. K. (2002). Representation of the Quantity of Visual
582 Items in the Primate Prefrontal Cortex. *Science, 297*(5587), 1708–
583 1711. https://doi.org/10.1126/science.1072493

584 Nieder, A., & Miller, E. K. (2003). Coding of Cognitive Magnitude: Compressed Scaling of
585 Numerical Information in the Primate Prefrontal Cortex. *Neuron*, *37*(1), 149–157.
586 https://doi.org/10.1016/S0896-6273(02)01144-3

587 Nieder, A., & Miller, E. K. (2004). A parieto-frontal network for visual numerical information
588 in the monkey. *Proceedings of the National Academy of Sciences, 101*(19), 7457–
589 7462. https://doi.org/10.1073/pnas.0402239101

590 Nieder, A. (2005). Counting on neurons: the neurobiology of numerical competence. *Nature*
591 *Reviews Neuroscience, 6*(3), 177–190. https://doi.org/10.1038/nrn1626

592 Nieder, A., Diester, I., & Tudusciuc, O. (2006). Temporal and Spatial Enumeration Processes
593 in the Primate Parietal Cortex. Science, 313(5792), 1431–
594 1435. https://doi.org/10.1126/science.1130308

595 Nieder, A., & Dehaene, S. (2009). Representation of Number in the Brain*. Annual Review of*
596 *Neuroscience, 32*(1), 185–208. https://doi.org/10.1146/annurev.neuro.051508.135550

597 Nieder, A. (2016). The neuronal code for number. *Nature Reviews. Neuroscience*, *17*(6), 366–
598 82. http://doi.org/10.1038/nrn.2016.40

599 Nieder, A. (2017). Magnitude Codes for Cross-Modal Working Memory in the Primate Frontal
600 Association Cortex, *Frontiers in Neuroscience, 11,* 1–7.
601 http://doi.org/10.3389/fnins.2017.00202

602 Oldfield, R. C. (1971). The assessment and analysis of handedness: The Edinburgh inventory.
603 *Neuropsychologia*, *9*(1), 97–113. http://doi.org/10.1016/0028-3932(71)90067-4

604 Ostwald, D., Schneider, S., Bruckner, R., & Horvath, L. (2019). Power, positive predictive
605 value, and sample size calculations for random field theory-based fMRI inference.
606 *bioRxiv*, 613331. https://doi.org/10.1101/613331

607 Piazza, M., Izard, V., Pinel, P., Le Bihan, D., & Dehaene, S. (2004). Tuning Curves for
608 Approximate Numerosity in the Human Intraparietal Sulcus. *Neuron, 44*(3), 547–
609 555. https://doi.org/10.1016/j.neuron.2004.10.014

610 Piazza, M., Mechelli, A., Price, C. J., & Butterworth, B. (2006). Exact and approximate
611 judgements of visual and auditory numerosity: An fMRI study. *Brain Research, 1106*(1),
612 177–188. https://doi.org/10.1016/j.brainres.2006.05.104

613 Piazza, M., Pinel, P., Le Bihan, D., & Dehaene, S. (2007). A Magnitude Code Common to
614 Numerosities and Number Symbols in Human Intraparietal Cortex. *Neuron, 53*(2), 293–
615 305. https://doi.org/10.1016/J.NEURON.2006.11.022

616 Piazza, M., & Izard, V. (2009). How Humans Count: Numerosity and the Parietal Cortex. *The*
617 *Neuroscientist, 15*(3), 261–273. https://doi.org/10.1177/1073858409333073

618 Plaisier, M.A., Bergmann Tiest, W. M., & Kappers, A. M. L. (2009). One, two, three, many -
619 Subitizing in active touch. *Acta Psychologica, 131*. 163–170.
620 doi:10.1016/j.actpsy.2009.04.003.

621 Plaisier, M.A., Bergmann Tiest, W. M., & Kappers, A. M. L. (2010). Range dependent
622 processing of visual numerosity: similarities across vision and haptics. *Experimental*
623 *Brain Research, 204*. 525–537. doi:10.1007/s00221-010-2319-y. PMC 2903696.

624 Plaisier, M.A., & Smeets, J. B. J. (2011). Haptic subitizing across the fingers. *Attention,*
625 *Perception, & Psychophysics, 73*. 1579–1585. doi:10.3758/s13414-011-0124-8. PMC
626 3118010.

627 Riggs, K.J., Ferrand, L., Lancelin, D., Fryziel, L., Dumur, G., & Simpson, A. (2006). Subitizing in
628 tactile perception. *Psychological Science, 17*(4). 271–272. doi:10.1111/j.1467-
629 9280.2006.01696.x. PMID 16623680.

630 Romo, R., Brody, C. D., Hernández, A., & Lemus, L. (1999). Neuronal correlates of parametric
631 working memory in the prefrontal cortex. Nature, 399(6735), 470–
632 473. https://doi.org/10.1038/20939

633 Schmidt, T. T., Wu, Y.H., & Blankenburg, F. (2017). Content-specific codes of parametric
634 vibrotactile working memory in humans. *Journal of Neuroscience*. 37(40), 9771-9777.
635 http://doi.org/10.1523/JNEUROSCI.1167-17.2017

636 Sperling, G. (1960). The information available in brief visual presentations. *Psychological*
637 *Monographs: General and Applied, 74*(11), 1-29.

638 Spitzer, B., Wacker, E., & Blankenburg, F. (2010). Oscillatory correlates of vibrotactile
639 frequency processing in human working memory. *The Journal of Neuroscience : The*
640 *Official Journal of the Society for Neuroscience*, *30*(12), 4496–502.
641 http://doi.org/10.1523/JNEUROSCI.6041-09.2010

642 Spitzer, B., & Blankenburg, F. (2011). Stimulus-dependent EEG activity reflects internal
643 updating of tactile working memory in humans. *Proceedings of the National Academy of*
644 *Sciences of the United States of America*, *108*(20), 8444–9.
645 http://doi.org/10.1073/pnas.1104189108

646 Spitzer, B., & Blankenburg, F. (2012). Supramodal parametric working memory processing in
647 humans. *The Journal of Neuroscience : The Official Journal of the Society for*
648 *Neuroscience, 32(10),* 3287–95. http://doi.org/10.1523/JNEUROSCI.5280-11.2012

649 Spitzer, B., Fleck, S., & Blankenburg, F. (2014a). Parametric alpha- and beta-band signatures
650 of supramodal numerosity information in human working memory. *The Journal of*
651 *Neuroscience : The Official Journal of the Society for Neuroscience*, *34*(12), 4293–302.
652 https://doi.org/10.1523/JNEUROSCI.4580-13.2014

653 Spitzer, B., Gloel, M., Schmidt, T. T., & Blankenburg, F. (2014b). Working memory coding of
654 analog stimulus properties in the human prefrontal cortex. *Cerebral Cortex, 24*(8),
655 2229–36. https://doi.org/10.1093/cercor/bht084

656 Tian, Y. & Chen, L. (2018). Cross-modal attention modulates tactile subitizing but not tactile
657 numerosity estimation. *Attention, Perception, & Psychophysics, 80*. 1229.
658 https://doi.org/10.3758/s13414-018-1507-x

659 Tudusciuc, O., & Nieder, A. (2009). Contributions of Primate Prefrontal and Posterior Parietal
660 Cortices to Length and Numerosity Representation. *Journal of Neurophysiology, 101*(6),
661 2984–2994. https://doi.org/10.1152/jn.90713.2008

662 Uluç, I., Schmidt, T. T., Wu, Y.-H., & Blankenburg, F. (2018). Content-specific codes of
663 parametric auditory working memory in humans. *NeuroImage, 183*.
664 https://doi.org/10.1016/j.neuroimage.2018.08.024

665 Vergara, J., Rivera, N., Rossi-Pool, R., & Romo, R. (2015). A Neural Parametric Code for
666 Storing Information of More than One Sensory Modality in Working Memory. *Neuron*,
667 *89*(1), 54–62. http://doi.org/10.1016/j.neuron.2015.11.026

668 von Lautz, A. H., Herding, J., Ludwig, S., Nierhaus, T., Maess, B., Villringer, A., & Blankenburg,
669 F. (2017). Gamma and Beta Oscillations in Human MEG Encode the Contents of
670 Vibrotactile Working Memory. *Frontiers in Human Neuroscience, 11,*
671 576. https://doi.org/10.3389/fnhum.2017.00576

672 Wu, Y., Uluç, I., Schmidt, T. T., Tertel, K., Kirilina, E., & Blankenburg, F. (2018). Overlapping
673 frontoparietal networks for tactile and visual parametric working memory
674 representations. *NeuroImage*, *166*, 325–334.
675 https://doi.org/10.1016/J.NEUROIMAGE.2017.10.059

676 Young, A.W., Bion, P.J. (1979). Hemispheric laterality effects in the enumeration of visually
677 presented collections of dots by children. *Neuropsychologia 17*, 99–102.

678

679

680 **Legends**

681 **Figure 1.** Sample pulse sequences and experimental paradigm **A.** Sample Stimuli. Pulse
682 sequences of 7, 9, 11 and 13 were used as experimental stimuli. For each numerosity, there
683 were four different durations (960, 1020, 1080 and 1140 ms), where each duration was sub-
684 divided into 60 ms slots. The distribution of pulses to slots was randomized for each stimulus
685 presentation. The first and the last slot of each stimulus always contained a pulse. The
686 stimuli displayed are for illustrative purposes. **B.** Experimental paradigm. A delayed-match-
687 to-numerosity task was employed, where two sample stimuli and a mask were presented
688 consecutively. A visual retro-cue presented simultaneously with the mask indicated which of
689 the numerosities should be retained for the 12 s delay. After the delay, participants
690 performed a two-alternative forced-choice, indicating which of the two test stimuli had the
691 same numerosity as the cued stimulus. The response period was 1.5 s. Please note that the
692 stimulus duration and inter-stimulus-interval changed depending on the stimulus duration,
693 but the onset of each event was locked to coincide with the onset of an image acquisition.
694
695 **Figure 2. A.** Mean rate of correct responses across participants (n = 34) for different
696 numerosities in main WM DMTN task. The figure shows that the WM performance
697 decreases with increasing numerosity. Error bars represent standard deviation (SD).
698 Asterisks indicate statistical significance for pair-wise t-tests, Bonferroni corrected for
699 multiple comparisons ($p < 0.05/6$). **B.** Mean performance across subjects for estimated
700 numerosity in number naming task (mean ± SD). **C.** True numerosities vs. mean numerosity
701 estimations (error bars show SD).
702

Figure 3. A. Brain regions coding information for the memorized estimated numerosities. Group level results of a t-contrast testing the 12 s WM delay for above chance prediction accuracy. Brain regions carrying information about memorized scalar magnitudes are: IFG = inferior frontal gyrus, MFG = middle frontal gyrus, PMC = premotor cortex, SMA = supplementary motor area, SFG = superior frontal gyrus. **B.** Time-courses of decoding accuracies of remembered (red) and non-remembered (grey) stimuli for all identified brain regions in the main analysis (Fig. 3A). Error bars indicate standard error. The figure shows that, for all clusters depicted in the main analysis, there is more numerosity-specific WM information for the remembered than forgotten numerosity and the information is present throughout the WM delay period. **C.** Results of the label-permutation tests. 5 bars are shown for each brain region, respectively. Each bar displays the mean prediction accuracy estimated from the distance to correct order groups. The shade of the bar color, ranging from black to white, depicts the different distance to correct ordering. Black bars indicate the mean prediction performance of the group with the correct linear order, while white bars represent the mean prediction accuracy derived from the most linearly unordered data. Brain regions tested for label permutation are: IFG = inferior frontal gyrus, MFG = middle frontal gyrus, PMC = premotor cortex, SMA = supplementary motor area, SFG = superior frontal gyrus. Error bars indicate standard error of the mean.

Table 1

Anatomical label and MNI coordinates of brain areas depicting memorized numerosity information during WM. All results are reported at $p_{FWE\text{-}Cluster} < 0.05$ with a cluster-defining threshold of $p < 0.001$. Mean prediction accuracy over the delay period is reported. Areas were, where possible, identified using the SPM anatomy toolbox (Eickhoff et al., 2005). IFG = inferior frontal gyrus, MFG = middle frontal gyrus, PMC = premotor cortex, MI = primary motor cortex, SMA = supplementary motor area, SFG = superior frontal gyrus.